Polish J. Chem., **75**, 1147–1169 (2001)

REVIEW ARTICLE

^{31}P High Resolution Solid State NMR Studies of Phosphoroorganic Compounds of Biological Interest*

by M.J. Potrzebowski, K. Ganicz and S. Kaźmierski

Polish Academy of Sciences, Center of Molecular and Macromolecular Studies, Sienkiewicza 112, 90-363 Łódź, Poland
E-mail marekpot@bilbo.cbmm.lodz.pl

In this review several applications of ^{31}P high resolution solid state NMR spectroscopy in structural studies of bioorganic samples is reported. The problem of pseudopolymorphism of bis[6-O,6′-O-(1,2:3,4-diisopropylidene-α-D-galactopyranosyl) phosphorothioyl] disulfide **1** and application of ^{31}P CP/MAS experiment to investigate of this phenomenon is discussed. The influence of weak C–H···S intermolecular contacts on molecular packing of 1,6-anhydro-2-O-tosyl-4-S-(5,5-dimethyl-2-thioxa-1,3,2-dioxaphosphorinan-2-yl)-β-D-glucopyranose **2** and S_P, R_P diastereomers of deoxy*xylo*thymidyl-3′-*O*-acetylthymidyl (3′,5′)-*O*-(2-cyanoethyl) phosphorothioate **3** and their implication on ^{31}P NMR spectra is shown. The final part of review describes the recent progress in structural studies of O-phosphorylated amino acids (serine, threonine, tyrosine), relationship between molecular structure and ^{31}P chemical shift parameters δ_{ii} and influence of hydrogen bonding on values of principal elements of chemical shift tensor.

Key words: structural studies, solid state NMR, pseudopolymorphism, intermolecular contacts, carbohydrate derivatives, phosphorylated amino acids, chemical shift tensor, hydrogen bonding

Introduction

In recent years the NMR spectroscopy has become one of the most powerful methods for structural studies of all kinds of solids including single crystals, crystalline powders, amorphous powders and glasses [1,2,3]. It is a result of introduction by Schaefer and Stejskal in 1976 the new experimental approach combining three techniques; cross-polarization of magnetization from abundant spin to "rare" spin, sample spinning under magic angle (54.7°) and high-power proton decoupling [4]. By means of the CP/MAS technique which leads to averaging or reducing the interactions of spin with magnetic field it is possible now to record the high resolution "liquid-like" spectra of solids. Moreover, Solid State NMR (SS NMR) spectroscopy is the technique that provides a link between NMR data in the solution or liquid phase and results obtained from single-crystal X-ray or neutron diffraction studies. Comparison of the isotropic chemical shifts and further structural results that characterize the geometry of molecules in the crystal lattice makes it is possible to draw conclusions regarding changes of conformation and configuration, as well as the nature of

*Dedicated to Prof. Jan Michalski on the occasion of his 80th birthday.

the intermolecular contacts in both phases. Since SS NMR uses a powder specimen (*i.e.* not only one selected single-crystal) this method can provide immediate polymorphs, solvates, inclusion complexes *etc*. that may exist in the crystalline state.

The ^{31}P nucleus is a very attractive probe for structural studies of phosporoorganic compounds because of the high sensitivity and 100% natural abundance [5,6,7]. In this review we describe the ^{31}P high resolution solid state NMR studies of bioorganic compounds containing phosphorus, carried out in NMR Laboratory of Polish Academy of Sciences in Łódź. The review is organized into the sections with Sections 2,3,4 providing the main body of the work. In Section 2 we discuss the problem of pseudopolymorphism of bis[6-O,6′-O-(1,2:3,4-diisopropylidene-α-D-galactopyranosyl) phosphorothioyl] disulfide **1** and application of ^{31}P CP/MAS experiment to investigate of this phenomenon. In Section 3 we show the influence of weak C–H···S intermolecular contacts on molecular packing of 1,6-anhydro-2-O-tosyl-4-S-(5,5-dimethyl-2-thioxa-1,3,2-dioxaphosphorinan-2-yl)-β-D-glucopyranose **2** and S_P, R_P diastereomers of deoxy*xylo*thymidyl-3′-*O*-acetylthymidyl (3′,5′)-*O*-(2-cyanoethyl) phosphorothioate **3** and their implication on ^{31}P NMR spectra. The Section 4 describes the recent progress in structural studies of O-phosphorylated amino acids (serine, threonine, tyrosine), relationship between molecular structure and ^{31}P chemical shift parameters δ_{ii} and influence of hydrogen bonding on values of principal elements of chemical shift tensors.

Investigation of pseudopolymorphism phenomenon of bis[6-O,6′-O-(1,2:3,4-diisopropylidene-α-D-galactopyranosyl) phosphorothioyl] disulfide 1

The *polymorphism* phenomenon is the existence of two or more crystalline forms of one compound. Polymorphs have a crystal structure with different packing of the same kind of molecules [8]. When solvent molecules are included in the crystal lattice such crystals contain more than one chemical entity and cannot be classified as polymorphs. This kind of crystals has been called *pseudopolymorphic*. According to the definition given by Desiraju and co-workers [9] "*Pseudopolymorphs are solvated forms of a compound which have different crystal structures and/or differ in the nature of the included solvent".* The terms like *solvate, inclusion compound* and *clathrate* depending on the chemical situation can also be used. In all these cases the existence of the higher-ordered structure is based on noncovalent interactions.

In our previous papers [10,11] we revealed that bis[6-O,6′-O-(1,2:3,4-diisopropylidene-α-D-galactopyranosyl) phosphorothioyl] disulfide **1** (Scheme 1) has very strong tendency to form *pseudopolymorphic* structures. Depending on the kind of the solvent used for crystallization, different crystallographic modifications of **1** can be obtained. As shown in Table 1, the structure of seven complexes was assigned by means of X-ray crystallography. Four of them crystallize in monoclinic crystallographic system, two in trigonal and one in orthorhombic system. For three solvates, containing different alcohol molecules (butanol, *n*-propanol and 2-propanol) in the crystal lattice of **1**, the space group was established to be C2. It is interesting to note

that each modification contains two molecules of solvents occluded in host lattice, however in case of **1e** one hexane and one benzene molecules are occluded.

Scheme 1

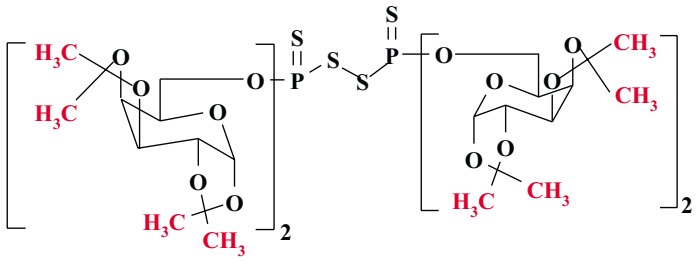

The differences of crystal and molecular structures of **1** are easily recognized by ^{31}P CP/MAS experiment, which provides complementary information into the contents and apparent symmetry of the crystallographic unit cell. The room temperature ^{31}P CP/MAS spectra of bis[6-O,6′-O-(1,2:3,4-diisopropylidene-α-D-galactopyranosyl) phosphorothioyl] disulfide crystallized under different conditions are displayed in Fig. 1a and Fig. 1b. The calculated values of principal tensors elements δ_{ii} and shielding parameters are given in Table 2.

At higher temperature the **1c** and **1d** are not stable and change of sample composition below the melting point is observed. Variable Temperature (VT) ^{31}P CP/MAS revealed that in both cases, owing to thermal processes, the spectra at 373 K became very similar and new modification **1h** is formed. Spectrum of **1h** (Figure 2) in the isotropic part is represented by two resonances separated by 3.0 ppm (86.3 ppm and 83.3 ppm). As concluded from ^{13}C CP/MAS spectra these changes are due to migration of solvent molecules from crystal lattice (Figure 3). With gradual increase of temperature, in range 300–370 K, the intensity of diagnostic signals of solvents (methyl groups of 2-propanol, $\delta_{^{13}C} = 26$ ppm, for **1c** and methyl $\delta_{^{13}C} = 30.5$ ppm and carbonyl group of acetone, $\delta_{^{13}C} = 204$ ppm, for **1d**) decreases.

Figure 4 shows how complicated is pathway from **1d** (Fig. 4a) to **1h** (Fig. 4d). Figures 4b and 4c display the ^{31}P CP/MAS spectra recorded at room temperature (only isotropic part) for sample **1d** kept 24 and 48 hours at 320 K under vacuum. From these studies it is apparent that migration of solvent causes significant changes of crystal lattice of host and the thermal phase reorientation of **1** is few-stage process. This conclusion can be extended to other pseudopolymorphs and is consistent with DSC studies. DSC profile for sample **1b** displayed in Figure 5 shows that **1b** release the guest molecules over a wide temperature range with the peak temperature 382.4 K respectively. This temperature is remarkably high in comparison to the boiling point of pure guest liquid (369.7 K for propanol), indicating that the guest molecules are strongly held within the crystal lattice.

Table 1. Crystallographic data for the pseudopolymorphs of bis[6-O,6′-O-(1,2:3,4-diisopropylidene-α-D-galactopyranosyl) phosphorothioyl] disulfide **1**.

	a	**b**	**c**	**d**	**e**	**f**	**g**
molecular formula	$C_{48}H_{76}O_{24}P_2S_4$ ×2($C_4H_{11}O$)	$C_{48}H_{76}O_{24}P_2S_4$ ×2(C_3H_8O)	$C_{48}H_{76}O_{24}P_2S_4$ ×2(C_3H_8O)	$C_{48}H_{76}O_{24}P_2S_4$ ×2(C_3H_6O)	$C_{48}H_{76}O_{24}P_2S_4$ ×2(C_6H_6)(C_6H_{14})	$C_{48}H_{76}O_{24}P_2S_4$ ×2(C_6H_6)	$C_{48}H_{76}O_{24}P_2S_4$ ×2($CHCl_3$)
M_r	1376	1348	1348	1343	1392	1384	1466
crystallization solvent	butanol	propanol	2-propanol	acetone	benzene/hexane	benzene	chloroform
crystallographic system	monoclinic	monoclinic	monoclinic	trigonal	orthorhombic	trigonal	monoclinic
space group	C2	C2	C2	$P3_2$	$P2_12_12_1$	$P3_2$	$P2_1$
a (Å)	29.529	29.386	29.412(1)	11.825(5)	10.536(4)	11.861(1)	10.4293(8)
b (Å)	10.433	10.430	10.429(1)	11.825(7)	25.067(4)	11.861(1)	28.206(2)
c (Å)	11.923	11.920	11.945(1)	43.082(9)	28.021(5)	44.679(3)	12.105(1)
α (°)	90.00	90.00		90.00			
β (°)	105.72	105.73	105.871(5)	90.00	90.00	90.00	90.696(8)
γ (°)	90.00	90.00		120.00			
V ($Å^3$)	3535.8	3516.7	3524(5)	5216.9(39)	7401(4)	5443(3)	3560.6(7)

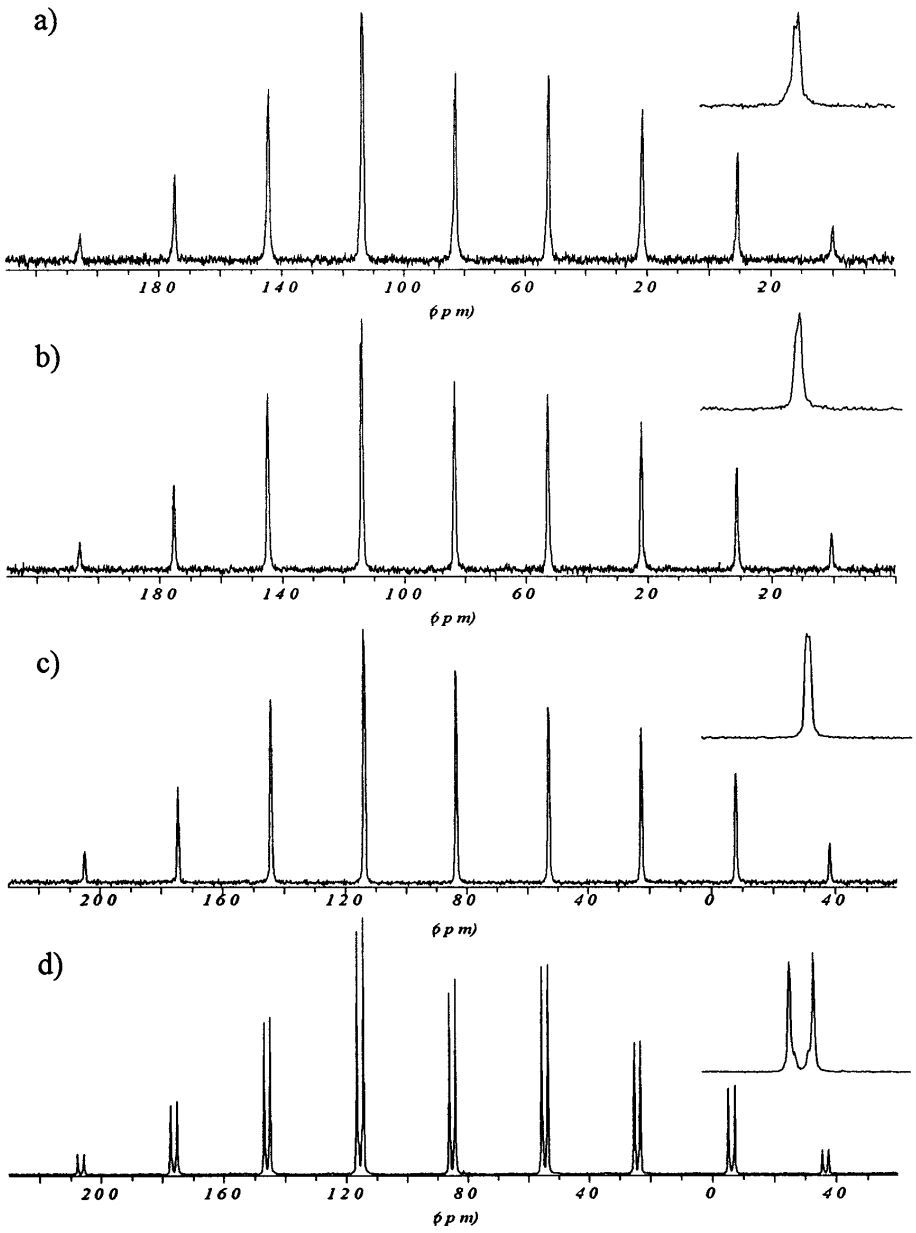

Figure 1a. 121.49 MHz ^{1}H-^{31}P CP/MAS experimental spectra of a) **1a** modification, b) **1b** modification, c) **1c** modification, d) **1d** modification. The spectra have 4 K data points with 10 Hz line broadening, a contact time of 1 ms, 100 scans and $\nu_{rot} = 3.7$ kHz.

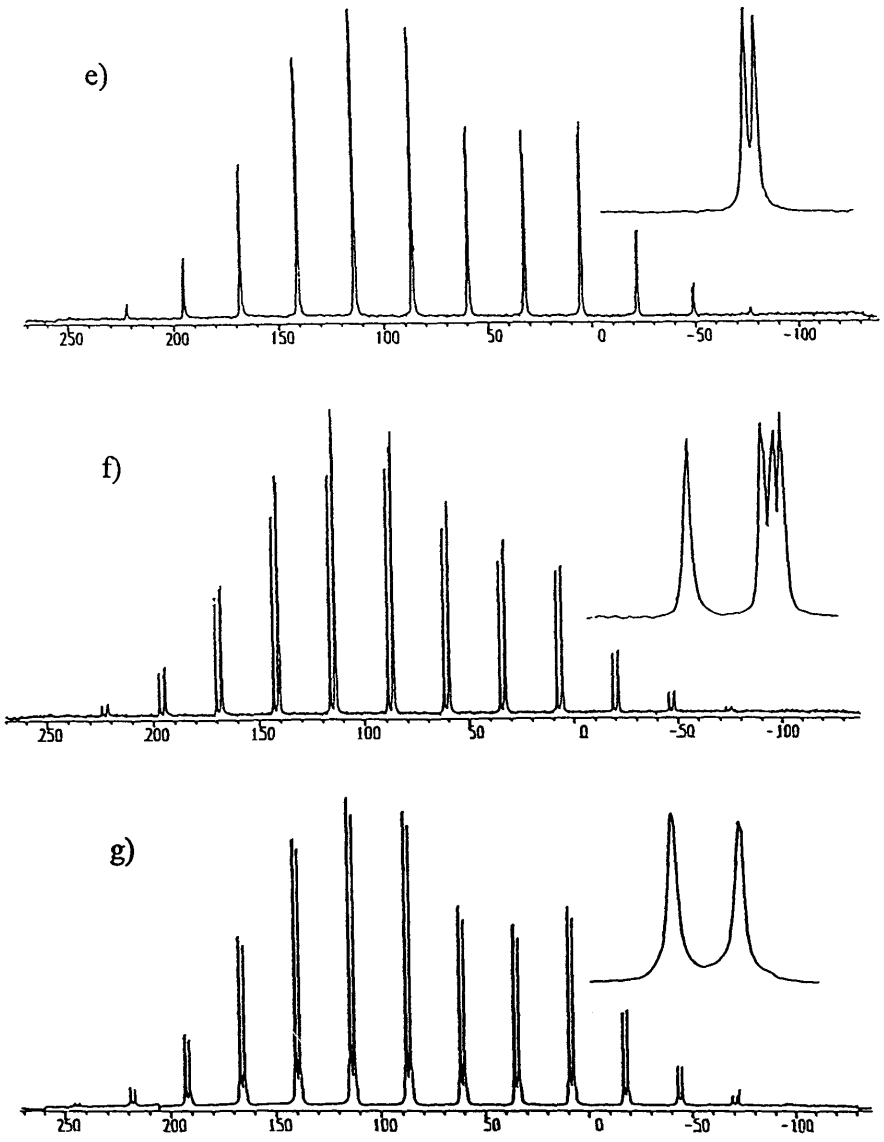

Figure 1b. 121.49 MHz ^{1}H-^{31}P CP/MAS experimental spectra of e) **1e** modification, f) **1f** modification, g) **1g** modification. The spectra have 4 K data points with 10 Hz line broadening, a contact time of 1 ms, 100 scans and ν_{rot} = 3.7 kHz.

Table 2. ^{31}P chemical shift parameters for bis[6-O,6′-O-(1,2:3,4-diisopropylidene-α-D-galactopyranosyl)-phosphorothioyl] disulfide **1**.

Modification (solvent)	δ_{iso} (ppm)	δ_{11} (ppm)	δ_{22} (ppm)	δ_{33} (ppm)	$\lvert\Delta\delta\rvert$ (ppm)	Ω (ppm)	η	κ
1a (n-butanol)	82.7	197.4	96.4	–45.9	193	243	0.79	0.17
1b (n-propanol)	83.4	199.1	96.4	–45.4	193	244	0.80	0.16
1c (2-propanol)	83.4	194.3	99.3	–43.2	190	238	0.75	0.20
1d	86.2	197.6	97.1	–36.0	183	234	0.82	0.14
(acetone)	84.2	191.2	91.5	–30.2	172	221	0.87	0.10
1e	86.8	196.6	105.0	–41.2	192	238	0.72	0.23
(benzene/hexane)	86.2	197.1	102.0	–40.7	190	237	0.75	0.20
1f	89.1	203.5	102.8	–39.1	192	242	0.79	0.17
(benzene)	86.8	189.9	104.7	–34.2	182	224	0.70	0.24
	86.5	199.7	101.8	–42.1	193	242	0.76	0.19
	86.1	196.6	103.6	–41.8	192	239	0.73	0.22
1g	88.0	200.2	103.2	–39.2	191	239	0.76	0.19
(chloroform)	85.9	200.4	96.2	–39.0	187	239	0.83	0.13

Estimated errors in δ_{11}, δ_{22} and δ_{33} are ± 2 ppm; errors in δ_{iso} are ± 0.2 ppm. The principal components of the chemical shift tensor are defined as follows: $\delta_{11} > \delta_{22} > \delta_{33}$. The isotropic chemical shift is given by $\delta_{iso} = (\delta_{11} + \delta_{22} + \delta_{33})/3$.

It is interesting to note that DSC profiles show not only endothermic peaks, which exhibit guest releasing but also apparent exothermic peaks which correspond to phase alternation. In particular, it is well seen for sample **1b**, where this effect is clearly cut**.** After releasing of the guest species, the crystals start to melt at 425 K giving the endothermic peak at 427 K. The understanding of the nature of the phase alternation is one of the most challenging questions in our future projects.

Continuing our interests in understanding the mechanism of solute-solvent interactions we investigated sample of **1** crystallized from n-propanol, acetone and methylcyclohexane. We have used perdeuterated solvents (2-propanol-d_8, acetone-d_6 and methylcyclohexane-d_{14}) to study motional behavior of the quest molecule in a crystal lattice. From inspection of Variable Temperature ^2H Quadecho experiment it is concluded that solvent molecules are loosely connected with the lattice of **1**. The fast molecular motion of solvent is slow down at low temperature (125 K); however, the molecules are still under fast regime exchange. At higher temperature (*ca* 350 K) the inclusion complexes undergo the phase reorientation and in the next step the migration of the solvent is observed.

Structural implications of C–H···S contacts in bioorganic phosphorothioyl compounds

Much attention has been paid to C–H···O hydrogen bonds as a factor affecting the structure of organic compounds and natural products [12,13]. The knowledge about the nature of weak interactions combined with known geometry of supramolecular synthons allows now to construct the supramolecular motifs in the solid phase [14].

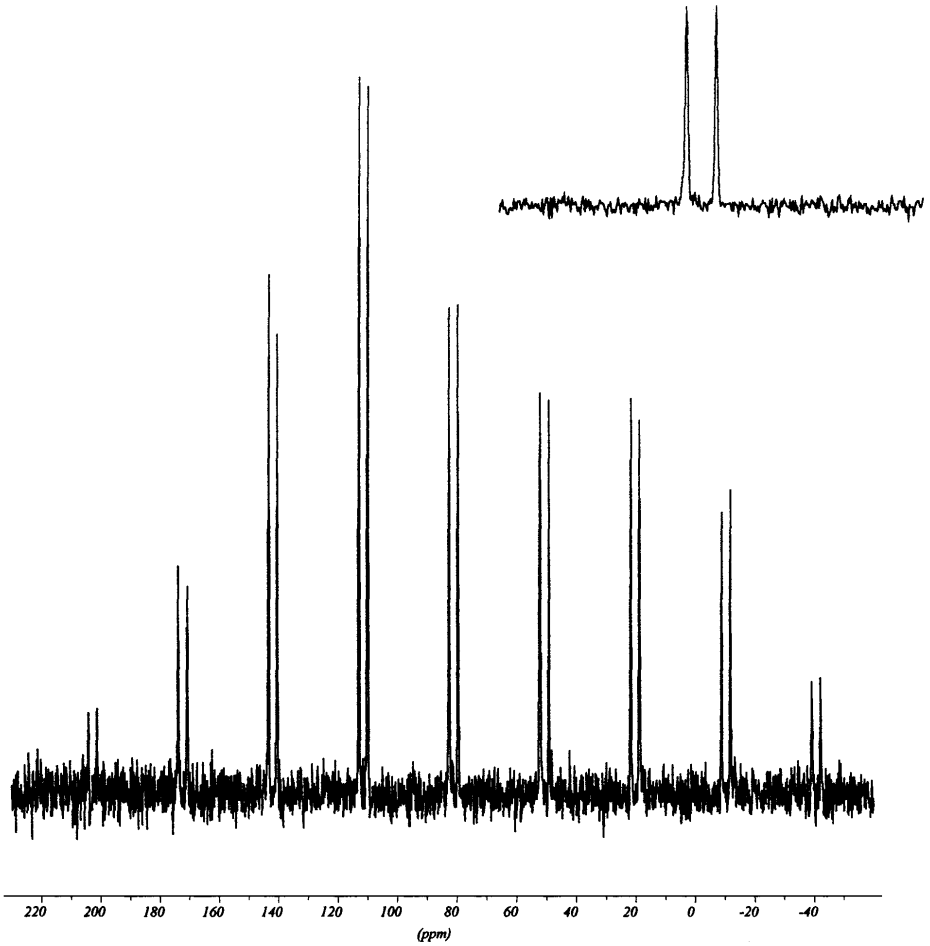

Figure 2. 121.49 MHz ^{1}H-^{31}P CP/MAS experimental spectra of **1h** modification.

After many years of controversy, the role of C–H···O contacts is no longer a matter of debate. Taylor and Kennard [15] showed that this type of interaction is electrostatic by nature and occur for C·····O distances between 3.0 and 4.0 Å assuming that the C–H····O angle is in the range 90°–180°. Its significance in crystal engineering was recently discussed by Desiraju [16,17]. Auffinger *et al*. have shown the importance of C–H···O hydrogen bonds in the molecular dynamics of anticodon hairpin of t-RNA [18]. To date less attention has been paid to C–H····S hydrogen bonds and this interaction has been rarely discussed in literature probably because of the two reasons. First, usually the other stronger interactions dominate the molecular packing and second the criteria applied for the recognition of a hydrogen bond based on van der Waals radii are rather restrictive. On the other hand, the significance of this type of interactions in the self-organization of crystals was discussed by Novoa *et al*. [19] and very recently by Persson, Sandström and coworkers [20].

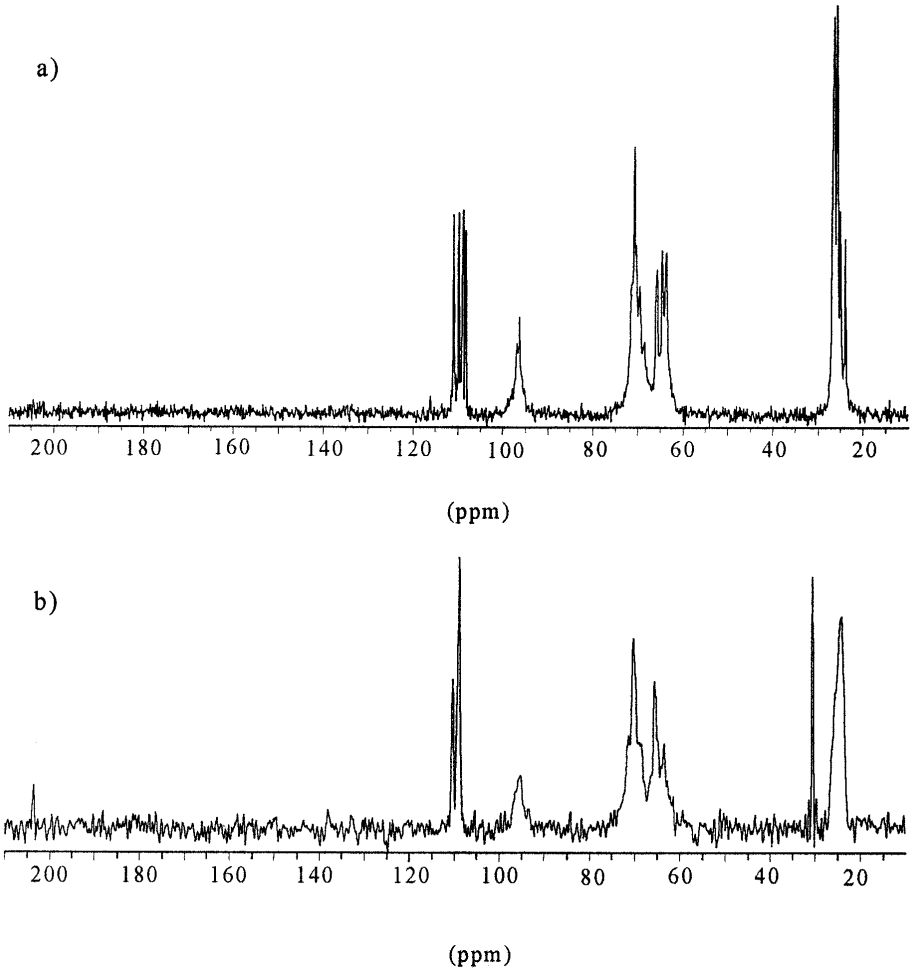

Figure 3. 75.46 MHz ^{1}H-^{13}C CP/MAS experimental spectra of a) **1c** modification, b) **1d** modification**.** The spectra have 4 K data points with 10 Hz line broadening, a contact time of 1 ms, 1 K scans and ν_{rot} = 3.7 kHz.

Searching the 1,6-anhydro-2-O-(tosyl)-4-S-(5,5-dimethyl-2-thioxa-1,3,2-dioxaphosphorinan-2-yl)-β-D-glucopyranose **2** (Scheme 2) in the solid phase we have found that C–H···S and C–H···O hydrogen bonds are one of the factors affecting the molecular packing [21]. The structure of different crystals formed by **2** was studied by X-ray crystallography and solid state NMR techniques. The room-temperature ^{31}P CP/MAS spectra of **2** crystallized from methanol **2a** and 2-propanol **2b** are displayed in Figure 6a and Figure 6b, respectively. Both spectra show a set of spinning sidebands from the large chemical shielding anisotropy (CSA). The principal components of the ^{31}P chemical shift tensors δ_{ii} were calculated from spinning sidebands

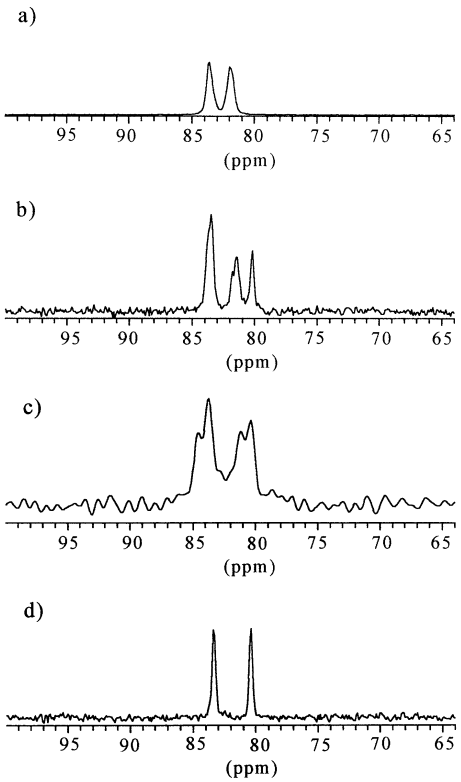

Figure 4. Isotropic part of the 121.49 MHz ^{1}H-^{31}P CP/MAS spectra of **1d** modification kept under vacuum at 320 K a) 1 hour, b) 24 hours, c) 48 hours, d) 5 days. The spectra have 4 K data points with 10 Hz line broadening, a contact time of 1 ms, 100 scans and ν_{rot} = 3.7 kHz.

intensities employing WIN-MAS program that is based on the Berger-Herzfeld algorithm [22,23]. The calculated values of principal tensors elements δ_{ii} and shielding parameters are given in Table 3. The accuracy of calculations was confirmed by comparison with theoretical spectra shown in Figure 6c and Figure 6d. The resemblance between the two spectra is apparent. The observed single lines in the isotropic part of the spectra are consistent with the X-ray data.

Scheme 2

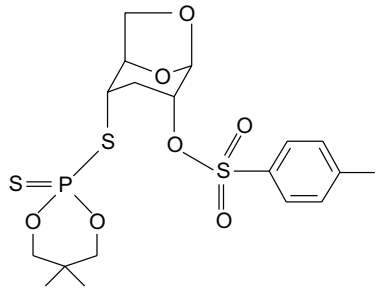

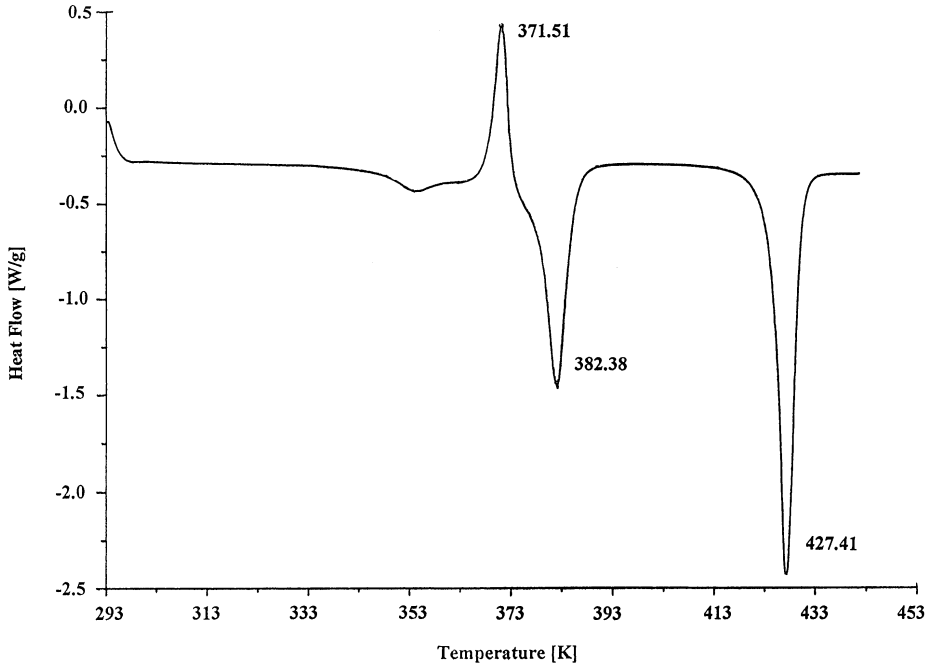

Figure 5. DSC profile of **1b** modification.

Table 3. ^{31}P chemical shift parameters for 1,6-anhydro-2-*O*-(tosyl)-4-S-(5,5-dimethyl-2-thioxa-1,3,2-dioxaphosphorinan-2-yl)-β-D-glucopyranose **2**.

Modification (solvent)	δ_{iso} (ppm)	δ_{11} (ppm)	δ_{22} (ppm)	δ_{33} (ppm)	$\lvert\Delta\delta\rvert$ (ppm)	Ω (ppm)	η	κ
2a (methanol)	87.5	185	140	–63	225	248	0.30	0.64
2b (2-propanol)	87.8	184	140	–61	223	245	0.30	0.64
2c (triturated from benzene with hexane)	87.7	183	141	–63	226	246	0.29	0.65
2d (toluene)	86.7	187	148	–75	243	262	0.24	0.70
	83.6	188	148	–85	253	273	0.23	0.71
2e (benzene/petrol ether)	89.1	193	145	–72	241	265	0.30	0.63
	87.5	186	141	–65	228	228	0.30	0.64
	84.6	186	146	–80	246	246	0.24	0.69

Estimated errors in δ_{11}, δ_{22} and δ_{33} are ± 2 ppm; errors in δ_{iso} are ± 0.2 ppm. The principal components of the chemical shift tensor are defined as follows: $\delta_{11} > \delta_{22} > \delta_{33}$. The isotropic chemical shift is given by $\delta_{iso} = (\delta_{11} + \delta_{22} + \delta_{33})/3$.

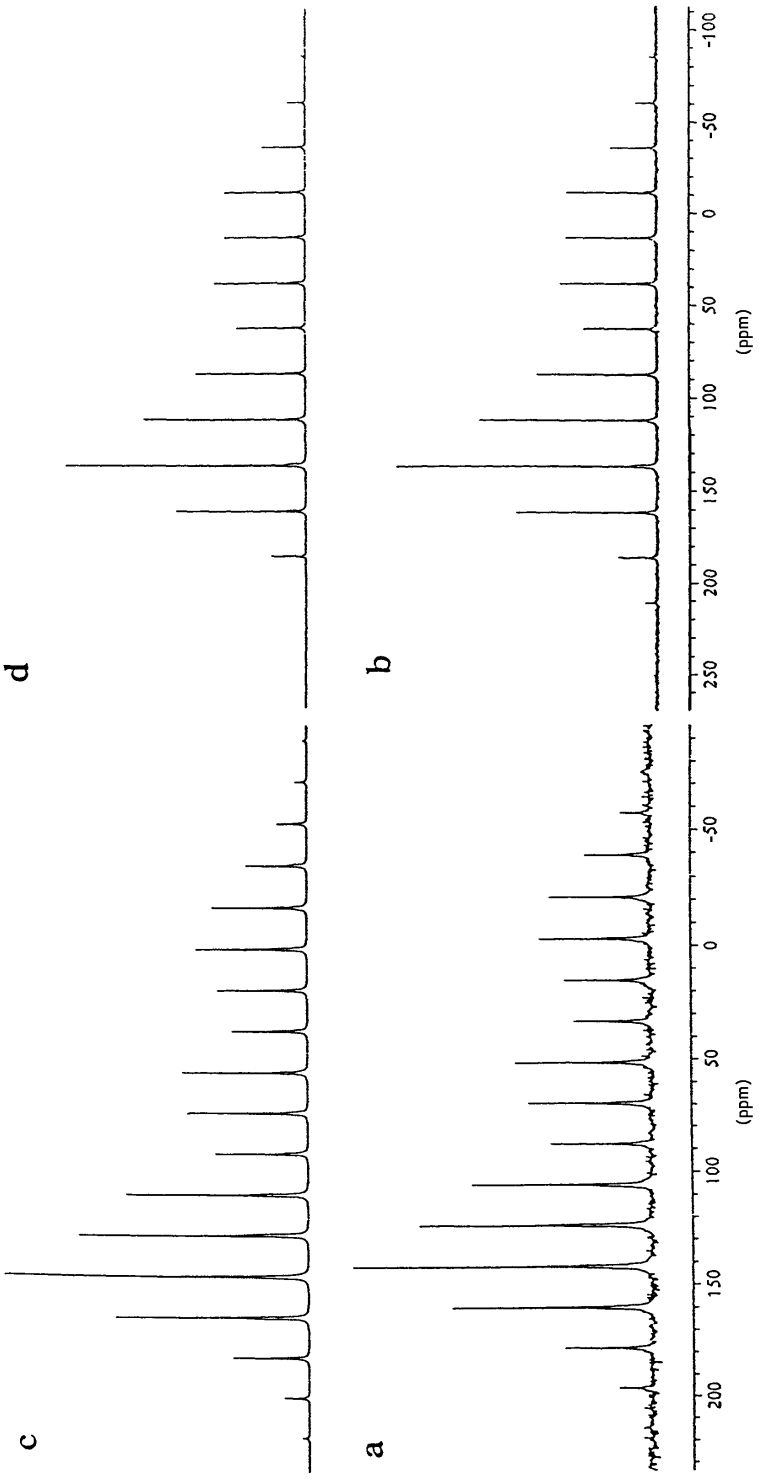

Figure 6. a) ^{1}H-^{31}P CP/MAS experimental spectrum of **2a**, ν_{rot} = 2.2 kHz. b) ^{1}H-^{31}P CP/MAS experimental spectrum of **2b**, ν_{rot} = 2.8 kHz. c) Theoretic spectrum of **2a**, d) Theoretic spectrum of **2b**. The experimental spectra have 8 K data points with a contact time 5 ms and 100 scans. Theoretic spectra were calculated employing the WIN-MAS program, version 940108, Bruker-Franzen Analytik GMBH, Bremen 1994.

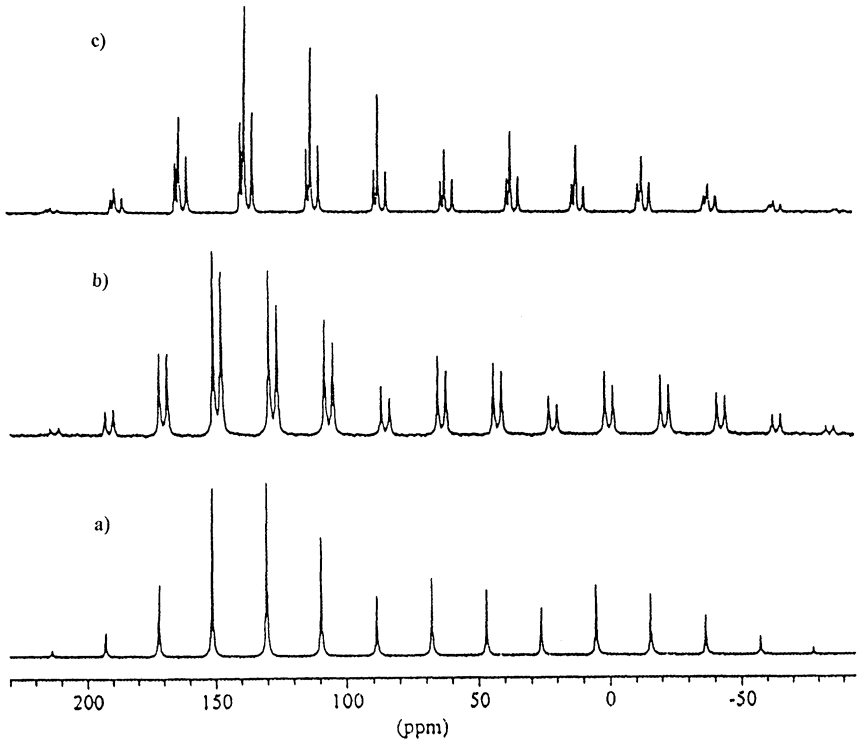

Figure 7. ^{1}H-^{31}P CP/MAS experimental spectra of **2** a) triturated from benzene with hexane-**2c**, b) crystallized from toluene- **2d**, c) crystallized from mixture benzene /petrol ether **2e**. All spectra have 8K data points, with a contact time 5 ms and 100 scans.

Figure 7a displays the **2c** (triturated from benzene employing hexane), while Figure 7b presents **2d** (crystallized from toluene) modification and Figure 7c shows **2** crystallized from mixture benzene/petrol ether (vol./vol.; 1/1) (**2e**). Each sample shows a different number of resonances in the isotropic part due to differences in packing of molecules in the crystal. The variable temperature (VT) ^{31}P CP/MAS experiment (Fig. 8) revealed that **2d** undergoes a phase transition below melting point (m.p. = 384 K).

Conclusions regarding the changes of geometry of the phosphorothioyl systems may be drawn from analysis of shielding parameters and ^{31}P principal components of chemical shift tensor, δ_{ii} [24,25]. Potrzebowski in series of bis(organophosphorothioyl) disulfides as well as Grossmann and coworkers employing *ab initio* IGLO calculations have shown that for dithiophosphoroorganic compounds δ_{33} parameter is oriented along P=S bond, whereas δ_{22} bisects the S=P–S plane [26,27]. Thus, the analysis of δ_{33} and δ_{22} parameters reflects the changes of the environment of phosphorus. The very detailed analysis of data collected in Table 3 shows several structural features of the **2**. For all modifications only small changes of δ_{11} and δ_{22} parameters (in the range of a few ppm) are seen. More significant differences are established for δ_{33} parameters and cover a range up to 20 ppm. For **2a** and **2b** the δ_{33} are upfield com-

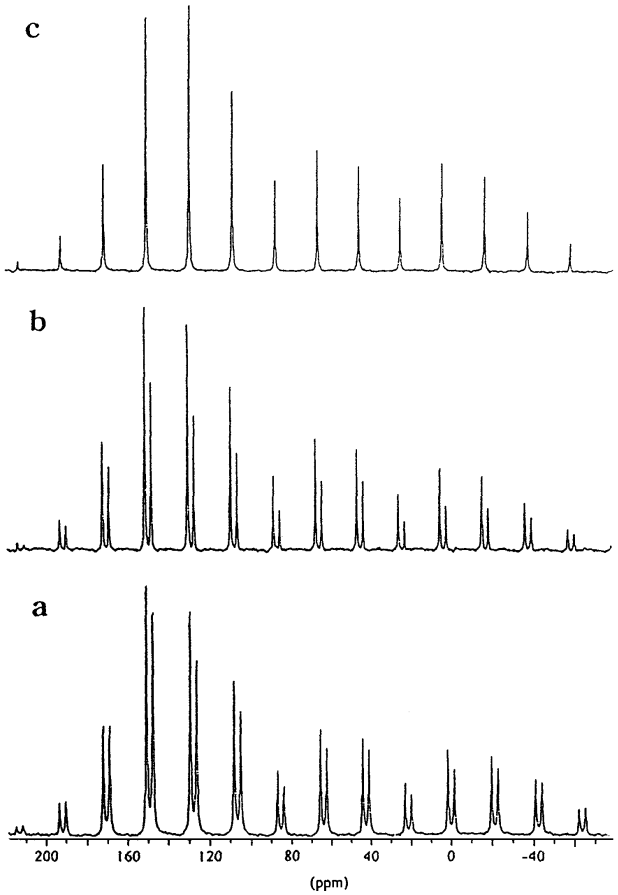

Figure 8. Variable temperature ^{31}P CP/MAS experimental spectra of **2d**. All spectra have 8 K data points, with a contact time 5 ms and 100 scans. a) at 298 K, b) at 338 K and c) at 378 K.

pared to modifications crystallized from benzene or toluene. Since for **2a** the P=S···H–C contacts are seen and for **2b** the solvent is hydrogen bonded to P=S unit, we assume that differences between δ_{33} values for **2a, 2b** and **2d** as well as other complexes are due to hydrogen bonding. The origin of this effect is related to the decrease in electronic shielding of the phosphorus as the phosphorothioyl group becomes more polarized during bond formation. The orientation of the δ_{ii} with respect to the molecular frame of the phosphorothioyl group concerning the hydrogen bond is shown in Scheme 3.

In our recent project describing the structural studies of diastereomers of deoxy-*xylo*thymidyl-3′-*O*-acetylthymidyl (3′,5′)-*O*-(2-cyanoethyl)phosphorothioate **3** (Scheme 4) in the solid state the significance of CH···S intermolecular contacts and their influence on molecular packing as well as changes of ^{31}P δ_{ii} parameters was considered [28]. Furthermore, ^{31}P SS NMR was used to optimize the crystallization condition, indication of the presence of different crystallographic modifications, and to establish ratio of crystalline *versus* amorphous phases.

The ^{31}P CP/MAS spectra of S_P-deoxy*xylo*thymidyl-3′-*O*-acetylthymidyl (3′,5′)-*O*-(2-cyanoethyl)phosphorothioate (S_P-**3**) crystallized from mixture of solvents are displayed in Figure 9. From inspection of spectrum 9a it is apparent that

Scheme 3

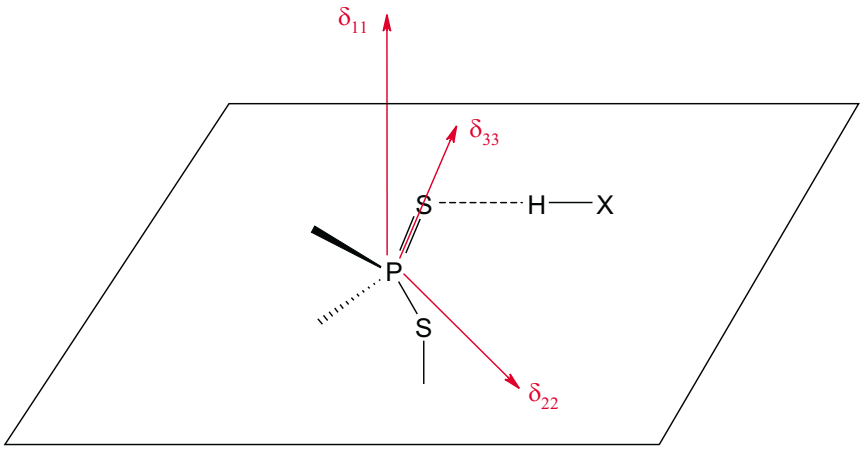

Scheme 4

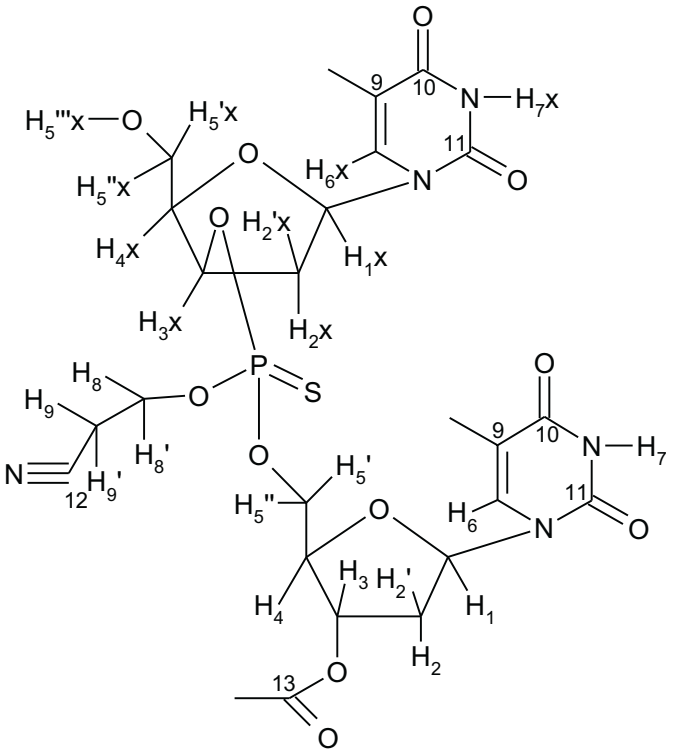

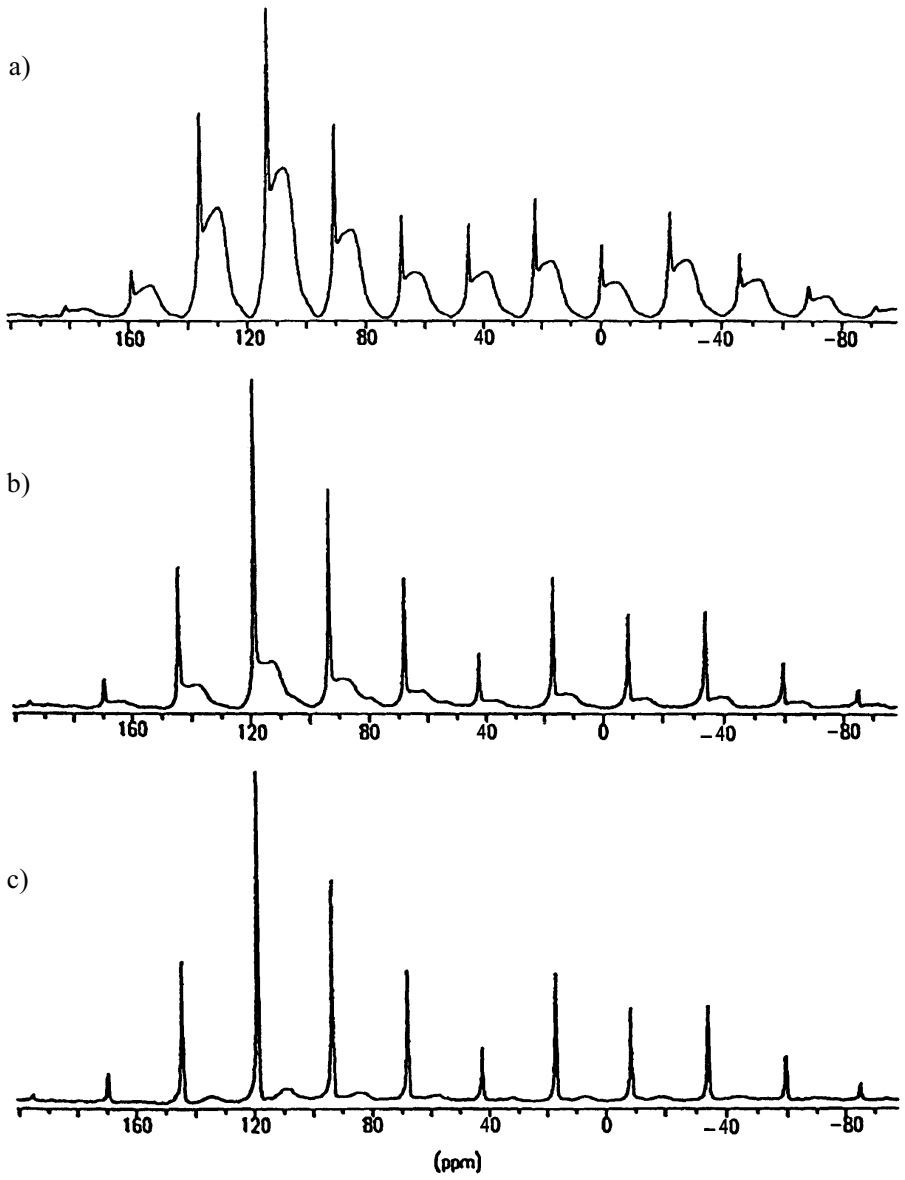

Figure 9. 121.49 MHz ^{1}H-^{31}P CP/MAS experimental spectra of S_P-**3**. The spectra have 4 K data points with 10 Hz line broadening, a contact time of 1 ms, 0.5 K scans and ν_{rot} = 2.7 kHz: a) spectrum recorded after first crystallization, b) spectrum after second crystallization with changed proportion of mixture of solvents, c) spectrum b recorded with dead time delay equal to $1/\nu_{rot}$.

powdered sample of S_P-**3** contains crystalline and amorphous phases in ratio *ca* 1:10 represented by sharp and very broad signals, respectively. As seen from spectrum 9b, with improved crystallization condition the proportion of both phases is changed. In

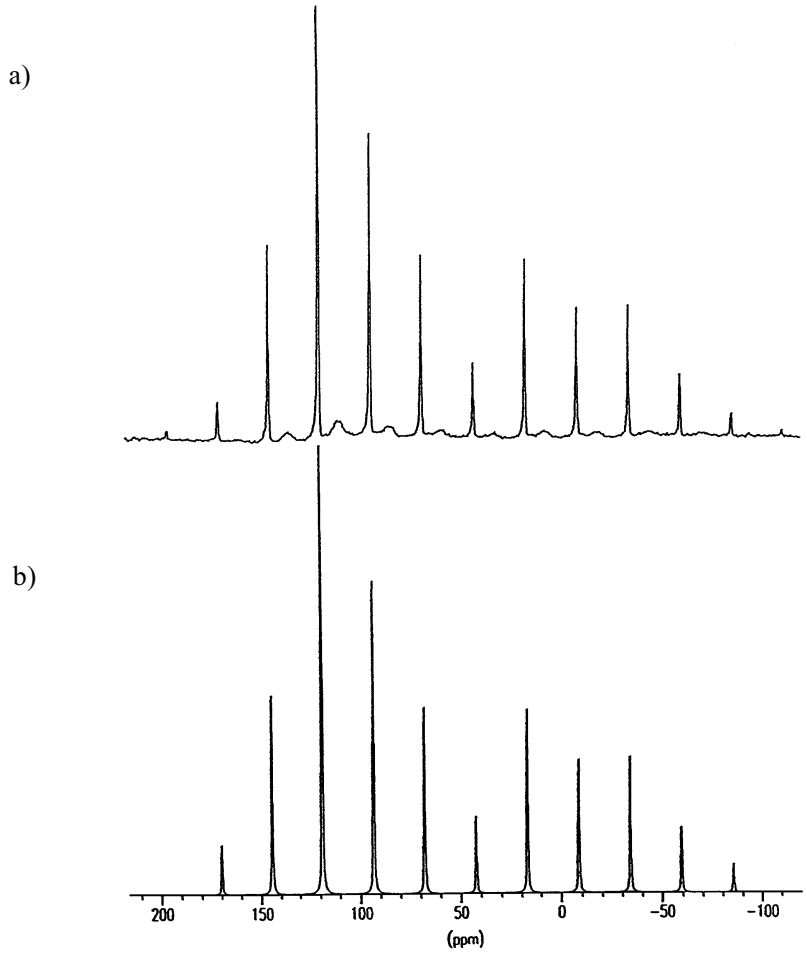

Figure 10. a) 121.49 MHz ^{1}H-^{31}P CP/MAS experimental spectrum of S_P-**3** recorded with conditions as given in Fig. 9c. b) Simulated spectrum calculated employing the WIN-MAS program, version 940108, Bruker-Franzen Analytik.

this work we were interested in analysis of principal elements of chemical shift for phosphorothioyl residue of dinucleotide in crystalline form and correlation between δ_{ii} parameters and molecular geometry. For this purpose, the good quality spectrum of crystalline phase was required. Taking advantage of differences in ^{31}P T_2 relaxation times of crystalline and amorphous phases the ^{31}P CP/MAS experiment was performed with "dead time delay" equal to 370 μs (one over rotor period at spinning rate 2700 Hz). Figure 9c presents the spectrum of sample S_P-**1** with almost completely eliminated signals from amorphous phase. Such spectrum was further used for theoretical calculations. The calculated values of principal tensors elements δ_{ii} and shielding parameters are given in Table 4. The accuracy of calculations was confirmed by comparison of experimental and theoretical spectra (Figure 10).

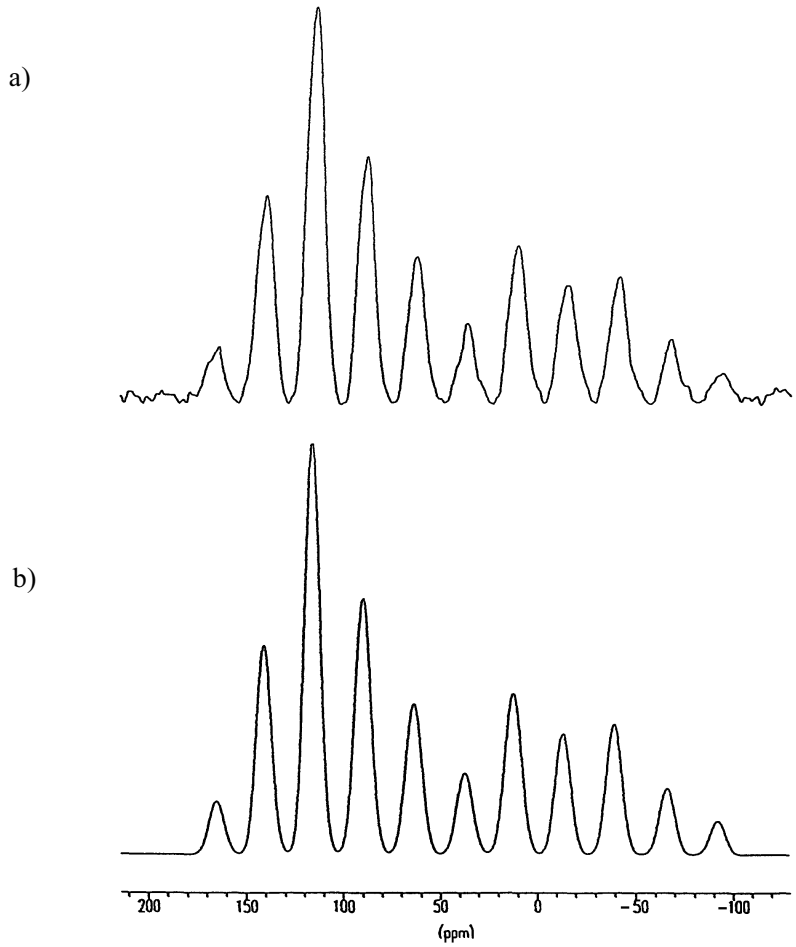

Figure 11. a) 121.49 MHz ^{1}H-^{31}P CP/MAS experimental spectrum of R_P-**3**. The spectrum has 4 K data points with 10 Hz line broadening, a contact time of 1ms, 0.5 K scans and ν_{rot} = 2.7 kHz. b) Simulated spectrum of R_P-**3** calculated employing the WIN-MAS program, version 940108, Bruker-Franzen Analytik.

Table 4. ^{31}P chemical shifts NMR parameters for $\boldsymbol{S_P}$-**3** and $\boldsymbol{R_P}$-**3**.

Compound	δ_{iso} (ppm)	δ_{11} (ppm)	δ_{22} (ppm)	δ_{33} (ppm)	$\lvert\Delta\delta\rvert$ (ppm)	Ω (ppm)	η	κ
$\boldsymbol{S_P}$-**3** (crystalline phase)	67.8	152	131	–81	223	233	0.14	0.81
$\boldsymbol{S_P}$-**3** (amorphous phase)	62.6	151	128	–91	230	242	0.20	0.81
$\boldsymbol{R_P}$-**3** (amorphous phase)	63.6	154	130	–92	233	246	0.16	0.85

Estimated errors in δ_{11}, δ_{22}, δ_{33} and $\Delta\delta$ are –/+5 ppm; errors in δ_{iso} are –/+0.2 ppm. The principal components of the chemical shift tensor are defined as follows: $\delta_{11} > \delta_{22} > \delta_{33}$. The isotropic chemical shift is given by $\delta_{iso} = (\delta_{11} + \delta_{22} + \delta_{33})/3$.

In contrast, attempts of crystallization of the R_P-**3** diastereomer provided only amorphous powder. Any strenuous attempts to obtain the crystals of R_P-**3** failed. Thus, the δ_{ii} elements were established only for amorphous form. The experimental and theoretical spectra are shown in Figure 11 and calculated parameters are collected in Table 4. The very detailed analysis of δ_{ii} shows several structural features S_P-**3** and R_P-**3**. It is interesting to note the considerable differences between isotropic values of crystalline and amorphous phases (~ 5 ppm). For all modifications only small changes of δ_{11} and δ_{22} parameters are seen. More significant differences are established for δ_{33} and cover the range up to 10 ppm. We have concluded that the effect is related to the formation of weak P=S····H–C hydrogen bonds and decrease in electronic shielding of the phosphorus as the phosphorothioyl group becomes more polarized during bond formation. Inspection of X-ray data for S_P-**3** shows several intra- and intermolecular P=S····H–C interaction. The most important intermolecular contacts seem to be interaction of sulfur with: *i)* CH_3 group of thymine, *ii)* CH_3 group of acyl block and *iii)* C(4)–H of deoxyribose.

In conclusion, examples described in this review and those found in CCDC show that C–H····S=P interactions are not unique. We have found more examples of the C–H····S=P contact than for the analogous C–H····O=P interactions. This fact can be explained in term of hard and soft hydrogen bonds. The S=P as a softer acceptor compared to O=P unit prefers to hydrogen bonding with the soft donor C–H. Such explanation is consistent with ideas of Carroll and Bader [29] who found a link between softness of an acceptor and character of hydrogen bonds and the recent results of Braga *et al*. who surveyed the hydrogen bonding in organometallic crystals [30]. The detailed analysis of the ^{31}P δ_{ii} principal elements of the chemical shift tensor suggests that distinction in values of δ_{33} parameters can be due to C–H····S=P interactions.

^{31}P CP/MAS NMR studies of O-phosphorylated amino-acids

Phosphorylation and dephosphorylation are one of the most important metabolic processes of living organism [31]. These processes involve replacement of hydroxyl group by phosphate residue (and *vice versa*) in numerous biologically active compounds as carbohydrates, nucleic acids and proteins [32]. In enzymatic reactions, the transfer proceeds *via* phosphorylation of OH function of serine, threonine or tyrosine. This process nearly always occurs on hydroxyl group of serine residue, however, the threonine and tyrosine are also involved. The incorporation of the phosphate group in the polypeptide chain may change its conformation and mode of the intermolecular interactions. Thus, there is a considerable interest in methods, which allow to investigate structural properties of this class of compounds both in liquid and solid state. The solid phase structure of O-phosporylated amino acids in enantiomeric and racemic form was systematically studied by means of the X-ray diffraction technique [33,34,35,36]. In contrast, to the best of our knowledge there are no similar studies for this class of compounds employing NMR methods.

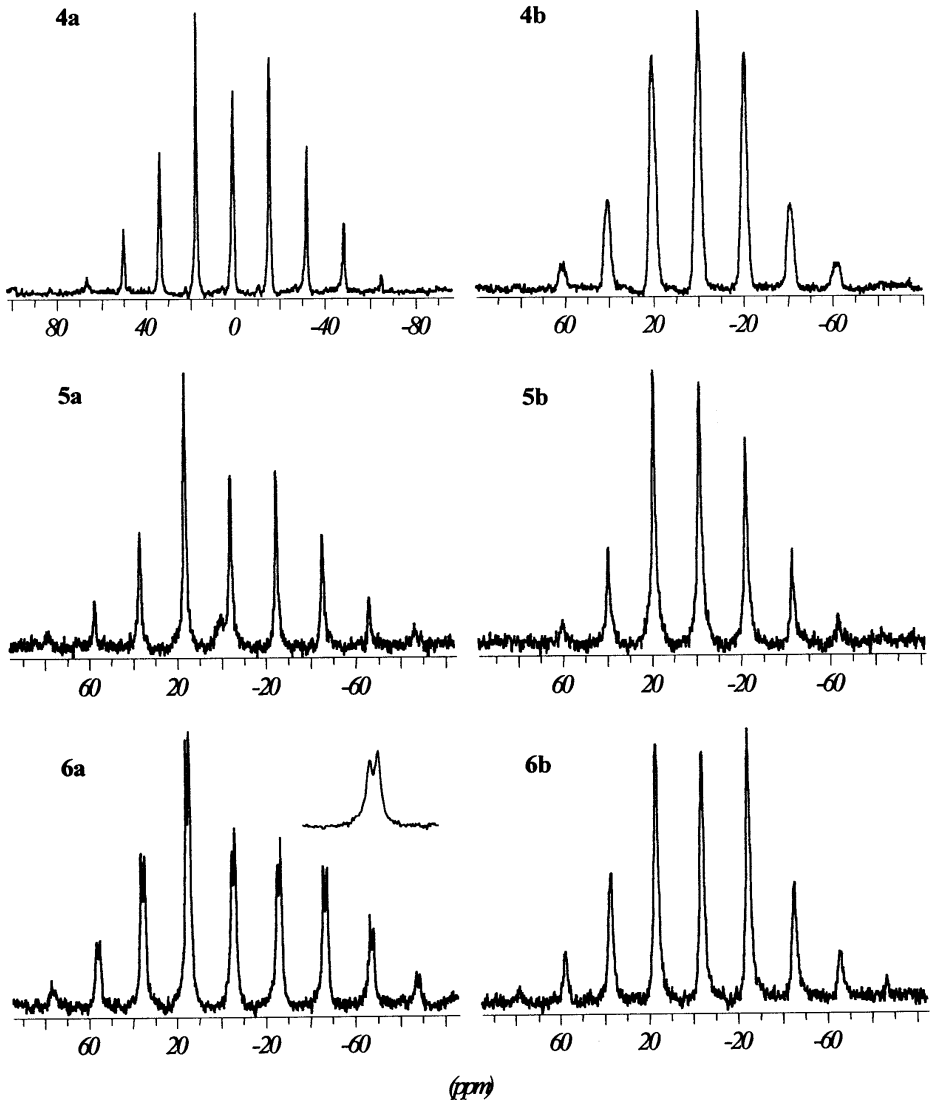

Figure 12. 121.49 MHz ^{1}H-^{31}P CP/MAS experimental spectra of phosphorylated amino acids; ν_{rot} = 2 kHz. **4a** – L-phosphoserine, **4b** – DL-phosphoserine, **5a** – L-phosphothreonine, **5b** – DL-phosphothreonine, **6a** – L-phosphotyrosine, **6b** – DL-phosphotyrosine.

In this review ^{31}P CP/MAS results for L and DL forms of three amino acids (phosphoserine **4**, phosphothreonine **5** and phosphotyrosine **6**) are shown. Figure 12 displays the ^{31}P CP/MAS spectra of samples **4a** (L-form)**, 4b** (DL-form)**, 5a** (L-form)**, 5b** (DL-form)**, 6a** (L-form)**, 6b** (DL-form)**,** recorded with spinning rate 2 kHz.

As seen compounds **4**, **5** and **6b** are represented by single resonances in the isotropic part of spectra. This result is consistent with X-ray data, which reveal that in case of **4** and **5** there is one independent molecule in the unit cell. There is no X-ray data for

sample **6b**, however, by analogy we can assume a similar crystal structure for this compound. For sample **6a**, ^{31}P CP/MAS studies unambiguously show that two molecules are asymmetric part of the unit cell. As in other cases, the analysis of principal elements of ^{31}P chemical shift tensor is a source of structural information. The ^{31}P δ_{ii} parameters established from spinning sideband analysis for **6a** and other phosphorylated amino acids are given in Table 5.

Table 5. ^{31}P chemical shift parameters for phosphorylated amino acids.

Phosphorylated amino acids		δ_{iso} (ppm)	δ_{11} (ppm)	δ_{22} (ppm)	δ_{33} (ppm)	Ω (ppm)	κ
4a	L-serine	0.1	50	2	–51	101	0.06
4b	DL-serine	–0.5	53	–5	–49	102	–0.13
5a	L-threonine	–4.5	58	7	–72	130	0.26
5b	DL-threonine	–2.2	50	1	–62	112	0.09
6a	L-tyrosine	–5.6	65	4	–89	154	0.19
		–7.2	60	1	–82	142	0.17
6b	DL-tyrosine	–4.6	59	–6	–68	127	0.03

Estimated errors in δ_{11}, δ_{22}, δ_{33} and $\Delta\delta$ are –/+5 ppm; errors in δ_{iso} are –/+0.2 ppm. The principal components of the chemical shift tensor are defined as follows: $\delta_{11} > \delta_{22} > \delta_{33}$. The isotropic chemical shift is given by $\delta_{iso} = (\delta_{11} + \delta_{22} + \delta_{33})/3$.

As seen, the anisotropy span parameters (Ω) are different and for instance for sample **4**, Ω is significantly smaller compared to sample **6a** (*ca* 50 ppm). It is well known that anisotropy parameter Ω reflect the distortion of molecular structure from ideal tetrahedral, whereas the asymmetry parameter κ corresponds to asymmetry of electron-density distribution about central atoms. In case of phosphate group the local environment of phosphorus is created by oxygen atoms. However, the bond length of P=O is significantly shorter compared to other. We assumed that hydrogen bonding strongly influence of geometry of phosphate residues and span parameter reflects the strength of hydrogen bonds. Putkey and Sundaralingman [33,34], employing X-ray technique, revealed very short phosphate-carboxyl hydrogen bond with distance between phosphate oxygen and the carboxyl group equal to 2.492 Å for O-phospho–L-serine as well as strong phosphate-phosphate contacts with very short P=O···O distance for DL form (**4b)**. Thus, the intermolecular effect is responsible for equalization of phosphorus-oxygen bonds and makes the phosphorus surrounding more symmetrical.

Comparing the δ_{ii} data collected in Table 5, the biggest difference is seen for δ_{33} elements. The orientation of δ_{ii} parameters with respect to molecular frame of phosphate group is known. As reported by Un and Klein [37] in phosphates δ_{11} parameter is oriented along longest P–O length, δ_{33} bisects the plane formed by the two shortest bonds and δ_{22} is perpendicular to plane formed by δ_{11} and δ_{33} (Scheme 5). However, as discussed elsewhere [37], the assignment of δ_{33} is ambiguous. It was speculated that differences of this element can reflect the changes of O=P–O valence angles or aver-

Scheme 5

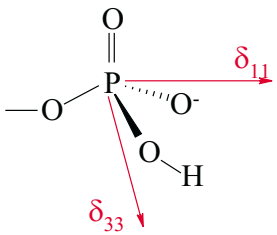

age length of shortest P–O bonds. We assume that intermolecular hydrogen bonding has influence on distinction of δ_{33} parameters. The project explaining the correlation of principal elements of ^{31}P chemical shift tensor with molecular structure of the phosphate group and intermolecular contacts on the ground of experimental methods and *ab initio* calculation is actually in progress.

Conclusions

In this review several applications of ^{31}P high resolution solid state NMR spectroscopy in structural studies of bioorganic samples are shown. As revealed this method can be used to investigate both molecular structure of particular phosphorus center as well as different kinds of the intermolecular contacts. The growing number of papers showing different applications of solid state NMR spectroscopy for investigation of very complex bioorganic compounds let state that this technique is about to undergo the kind of revolution that solution-state NMR underwent in 80-ties. New methodological approaches combined with *ab initio* calculation of NMR parameters show a prospective and very promising trend for structural studies of biomolecular systems.

Acknowledgment

The authors are indebted to the Polish State Committee for Scientific Research for financial support (grant no. 3T09A 026 19).

REFERENCES

1. Fyfe C.A., Solid State NMR for Chemists, Eds. CFC Press, Guelph, Ontario 1983.
2. Mehring M., Principles of High Resolution NMR in Solids, Springer, Berlin 1983.
3. Yannoni C.S., *Acc. Chem. Res*., **15**, 201 (1982).
4. Schaefer J. and Stejskal E.O., *J. Am. Chem. Soc*., **98**, 1031 (1976).
5. Gorenstein D.G., Phosphorus-31 NMR. Principles and Applications, Academic Press, Orlando 1984.
6. Van Wazer J.R., Phosphorus and its Compounds, Intersc. Publ., NY 1961.
7. Verkade J.G. and Quin L.D., Phosphorus-31 NMR Spectroscopy in Stereochemical Analysis, VCH Publ. Inc., Deerfield Beach 1987.
8. Glusker J.P., Lewis M. and Rossi M., Crystal Structure Analysis for Chemists and Biologists, VCH Publishers, Inc., NY 1994, p. 44.
9. Kumar V.S.S., Kuduva S.S. and Desiraju G.R., *J. Chem. Soc., Perkin Trans. 2*, 1069 (1999).

10. Potrzebowski M.J., Błaszczyk J. and Wieczorek M.W., *J. Org. Chem.,* **60**, 2549 (1995).
11. Potrzebowski M.J., Ganicz K., Ciesielski W., Skowrońska A., Wieczorek M.W., Błaszczyk J. and Majzner W., *J. Chem. Soc., Perkin Trans. 2*, 2163 (1999).
12. Sutor D.J., *Nature*, **68**, 195 (1962).
13. Sutor D.J., *J. Chem Soc.*, 1105 (1963).
14. Desiraju G.R., *Angew. Chem., Int. Ed. Engl.,* **34**, 2311 (1995).
15. Taylor R. and Kennard O., *J. Am. Chem. Soc.,* **104**, 5063 (1982).
16. Desiraju G.R., *Acc. Chem. Res.,* **24**, 290 (1991).
17. Desiraju G.R., *Acc. Chem. Res.,* **29**, 441 (1996).
18. Auffinger P., Louise-May S. and Westhof E., *J. Am. Chem. Soc.,* **118**, 1181 (1996).
19. Novoa J.J., Carme Rovira M., Rovira C. and Veciane J. Tarres, *J. Adv. Mater.,* **7**, 233 (1995).
20. Borrmann H., Persson I., Sandström M. and Stålhandske Ch.M.V., *J. Chem. Soc., Perkin Trans. 2,* 393 (2000).
21. Potrzebowski M.J., Michalska M., Kozioł A.E., Kaźmierski S., Lis T., Pluskowski J. and Ciesielski W., *J. Org. Chem.,* **63**, 4209 (1998).
22. WIN-MAS program, version 940108, Bruker-Franzen Analytik GMBH, Bremen 1994.
23. Herzfeld J. and Berger A., *J. Chem. Phys.,* **73**, 6021 (1980); Jeschke G. and Grossmann G., *J. Magn. Reson.,* 12**A103**, 323 (1993).
24. Potrzebowski M.J. and Michalski J., Phosphorus-31NMR Spectral Properties in Compound Characterization and Structural 12Analysis, Eds. L.D. Quin, J.G. Verkade, VCH 1994, p. 413.
25. Grossmann G., Beckmann H., Rademacher O., Krueger K. and Ohms G., *J. Chem. Soc., Dalton Trans.,* 2797 (1995).
26. Potrzebowski M.J., *J. Chem. Soc., Perkin Trans. 2*, 63 (1993).
27. Krüger K., Grossmann G., Fleischer U., Franke R. and Kutzelnigg W., *Magn. Reson. Chem.,* 33 (1995).
28. Potrzebowski M.J., Yang X., Misiura K., Majzner W.R., Wieczorek M.W., Kaźmierski S., Olejniczak S. and Stec W.J., *Eur. J. Org. Chem.,* 1491 (2001).
29. Carroll M.T. and Bader R.F.W., *Mol. Phys.,* **65**, 695 (1988).
30. Braga D., Grepioni F., Biradha K., Pedireddi V.R. and Desiraju G.R., *J. Am. Chem. Soc.,* **117**, 3156 (1995).
31. Corbridge D.E.C., Phosphorus, An Outline of Its Chemistry, Biochemistry and Technology, Elsevier, Amsterdam-Oxford-New York-Tokyo, 1990, p. 880.
32. Marseigne I. and Rogues B.P., *J. Org. Chem.,* **53**, 3621 (1988); Kitas E.A., Perich J.W., Tregear G.W. and Johns R.B., *J. Org. Chem.,* **55**, 4181 (1990).
33. Putkey E. and Sundaralingam M., *Acta Cryst.,* **B26**, 782 (1970).
34. Putkey E. and Sundaralingam M., *Acta Cryst.,* **B26**, 790 (1970).
35. Maniukiewicz W., Kwiatkowski W. and Blessing R.H., *Acta Cryst.,* **C52**, 1736 (1996).
36. Suga T., Inubushi C. and Okabe N., *Acta Cryst.,* **C54**, 83 (1998).
37. Un S. and Klein M.P., *J. Am. Chem. Soc.,* **111**, 5119 (1989).